

## Disrupting Fracture Toughness Of Adhesively Bonded Joints By Tailoring Composite Substrates

Lima, R. A. A.; Tao, R.; Teixeira De Freitas, S.

**Publication date**

2024

**Document Version**

Final published version

**Published in**

Proceedings of the 21st European Conference on Composite Materials

**Citation (APA)**

Lima, R. A. A., Tao, R., & Teixeira De Freitas, S. (2024). Disrupting Fracture Toughness Of Adhesively Bonded Joints By Tailoring Composite Substrates. In C. Binetruy, & F. Jacquemin (Eds.), *Proceedings of the 21st European Conference on Composite Materials: Volume 8 - Special Sessions* (Vol. 8, pp. 1010-1016). The European Society for Composite Materials (ESCM) and the Ecole Centrale de Nantes..

**Important note**

To cite this publication, please use the final published version (if applicable).  
Please check the document version above.

**Copyright**

Other than for strictly personal use, it is not permitted to download, forward or distribute the text or part of it, without the consent of the author(s) and/or copyright holder(s), unless the work is under an open content license such as Creative Commons.

**Takedown policy**

Please contact us and provide details if you believe this document breaches copyrights.  
We will remove access to the work immediately and investigate your claim.

## DISRUPTING FRACTURE TOUGHNESS OF ADHESIVELY BONDED JOINTS BY TAILORING COMPOSITE SUBSTRATES

R.A.A. Lima<sup>1</sup>, R. Tao<sup>1</sup>, S. Teixeira de Freitas<sup>1,2</sup>

<sup>1</sup> Faculty of Aerospace Engineering, Delft University of Technology, Delft, the Netherlands

Email: R.DeAraujoAlvesLima@tudelft.nl

R.Tao@tudelft.nl

<sup>2</sup> IDMEC, Instituto Superior Técnico, Lisbon, Portugal.

Email: sofia.teixeira.freitas@tecnico.ulisboa.pt

**Keywords:** Adhesive joints, tailoring, stacking sequence, toughening, multi-damage

### Abstract

This work aims to improve the damage tolerance of secondary adhesively bonded joints under quasi-static mode I loading conditions by architecting the carbon fibre-reinforced polymer substrates' stacking sequences [1]. Double Cantilever Beam tests show that architecting the stacking sequence of the laminates composite substrates in combination with the adhesive layer's fracture toughness affects the crack onset and triggers different crack paths throughout the joints' thickness. In specimens bonded with a low-toughness bi-component adhesive, the tailored design, including a co-cured toughening layer, could increase the effective fracture toughness of the composite bonded joints up to 200%. From this study, it was possible to recognise the complexity and benefits of moving from the traditional cohesive failure to outbreacking multiple crack path propagation.

### 1. Introduction

Increasing efforts to improve sustainability in the aeronautical industry have pushed the use of advanced lightweight materials such as Carbon Fibre Reinforced Polymers (CFRP) combined with high-strength alloys to produce lightweight structures. Adhesive bonding is one of the most suitable joining methods for assembling multi-materials and repairing composite structures. However, its application in primary structures with a high load-bearing capacity is limited to several safety restrictions. Since adhesive joints often present limited resistance to crack growth and sudden failure, and interface contamination cannot be detected with conventional nondestructive testing, secondary bonding of primary structures is not certified, and backup solutions (i.e. rivets) are mandatory.

However, rivets imply extra non-neglectable weight to the structures, contributing to additional fuel consumption. To increase adhesively bonded joints' safety and reliability and reach their full potential even in safety-critical applications, it is crucial to invest in new edge-cutting design solutions that improve their resistance against crack growth and avoid sudden failure.

The authors' previous work [1] exploited the effects of tailoring the stacking sequence of CFRP substrates in the effective fracture toughness of adhesively bonded Double Cantilever Beam (DCB) specimens tested under quasi-static mode I loading condition. Five stacking sequences and two types of adhesives with different ranges of fracture toughness were tested.

It was then shown that the ply angle orientation next to the bondline and the adhesive fracture toughness are relevant in triggering crack competition and the co-occurrence of multiple damage mechanisms (i.e. delamination, cohesive failure and transversal matrix cracking). In particular, the substrates with various fibre orientation angles ( $[90/45/-45/0]_s$  and  $[90/60/90/-60/0]_s$ ) increased their effective fracture toughness every time the crack deflected to a different ply throughout the substrate thickness. This

behaviour is continuous until the crack deflects to the next 0-degree ply when a drop in the effective fracture toughness and final delamination is observed.

The tailoring of the substrate stacking sequence, particularly for non-toughened adhesives ( $G_{IC}$  around  $600 \text{ J/m}^2$ ), seems a promising solution to increase the effective fracture toughness of the bonded joints. However, the final sudden delamination at the 0-degree layer is still a key challenge for implementation as a crack-arresting feature for adhesively bonded joints.

This research presents a novel solution to address this limitation of the final delamination step at the 0-degree ply by introducing an extra toughening layer of a toughened adhesive co-cured with the CFRP substrates.

The extra toughening layer was studied for two specific adhesive/CFRP layup combinations: (i) AF 163-2k –  $[0/90_2/0]_s$  and (ii) Araldite 2015/1 –  $[90/45/-45/0]_s$ . The aim is to understand the effects of implementing an extra toughening layer in the final fracture toughness of the proposed joints.

## 2. Materials and methods

### 2.1. Specimens manufacturing

The unidirectional CFRP Hexply 8552 – AS4 prepreg with toughened epoxy resin (Hexcel Composites, Cambridge - UK) was used to manufacture the DCB substrates. Two different adhesives were used to secondary bond the DCB specimens: (i) toughened adhesive with an embedded nylon carrier, AF 163-2K ( $G_{IC} = 2416 \text{ J/m}^2$ ) [2] – supplied by the 3M Scotch-Weld™, and (ii) a bi-component epoxy adhesive Araldite 2015/1 ( $G_{IC} = 640 \text{ J/m}^2$ ) [3] – supplied by Huntsman International LLC.

In addition, the adhesive AF 163-2k was used as the extra toughening layer co-cured in the new tailored substrate's layups. The following substrates stacking sequences were studied:  $[0/90_2/AF163-2k/0]_s$  and  $[90/45/-45/AF163-2k/0]_s$ , highlighting the presence of the toughening layer before the 0-degree ply.

The substrates were manufactured by hand layup of the prepreps previously cut at the specified fibre orientation angles. Intermediate debulking steps of 20 minutes between each added layer were performed in a sealed table under the constant pressure of around 100 mbar. The final CFRP laminates were then sealed in a vacuum bag and, finally, cured in an autoclave under 5 bars with a double dwell step: (i) at  $110^\circ\text{C}$  for 60 minutes and (ii) at  $180^\circ\text{C}$  for 120 minutes.

After cooling, the CFRP laminates were cut to the final dimensions of the DCB substrates. Both laminate types had their smooth surface side manually sanded with 400-grid sandpaper following a criss-cross pattern and cleaned with acetone. In addition, the UV/Ozone physical surface treatment was applied for 7 minutes on the surfaces to be bonded to remove thin layers of organic contaminants and improve the substrate's wettability, as detailed in [1,4,5].

The specimens  $[0/90_2/AF163-2k/0]_s$  were secondary bonded with the film adhesive AF 163-2k with a curing cycle in the autoclave with a total pressure equal to 3 bars at  $120^\circ\text{C}$  for 90 minutes. The specimens  $[90/45/-45/AF163-2k/0]_s$  were instead bonded with the bi-component epoxy adhesive Araldite 2015/1 and cured in an oven at  $80^\circ\text{C}$  for 60 minutes.

An initial crack length of 30 mm was ensured using a Teflon tape (thickness equal to 0.11 mm) on the bonded side of the substrates. The adhesive thickness and the specimen nomenclature are listed in Table 1.

Table 1: Specimens details and nomenclature.

Specimen type	Adhesive type	Adhesive thickness
[0/90 <sub>2</sub> /AF163-2k/0] <sub>s</sub>	AF 163-2k	0.25 mm – ensured by embedded carrier
[90/45/-45/AF163-2k/0] <sub>s</sub>	Araldite 2015/1	0.3 mm – ensured by metallic spacers

Finally, the specimens' metallic load blocks were bonded using the bi-component epoxy Araldite 2012. Figure 1 shows the specimen's schematic.

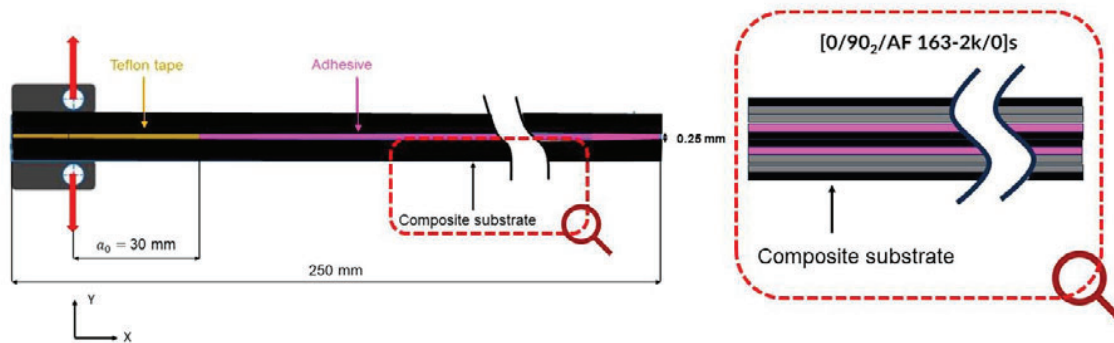


Figure 1: Schematic of specimen [0/90<sub>2</sub>/AF163-2k/0]<sub>s</sub>.

## 2.2. Experimental setup

The DCB quasi-static mode I tests were performed in a Zwick electro-mechanical testing machine with a load cell of 1 kN. The testing speed was equal to 4 mm/min, and at least three specimens were tested for each type, as recommended by ISO 25217 [6]. The load and displacement values from the tests were recorded at 10 Hz frequency.

The crack position was continuously tracked during the tests by visual inspection using a digital camera (5 Mpixel) of the white-painted lateral surface of the specimens. The free lateral surface of the DCB specimens was monitored using a travelling digital microscope to identify possible crack deflections. The digital camera and microscope had an acquisition frequency of 4 photos each second and were synchronised with the load-displacement signal outputs from the testing machine.

## 2.3. Data reduction method

The Modified Beam Theory (MBT) was used to determine the effective fracture toughness of the tailored DCB specimens, following the equation (Eq.1) below:

$$G_I = \frac{3P\delta}{2b(a + |\Delta|)} * \frac{F}{N} \quad (1)$$

In which the variables meaning are:

- $P$  – load [N];
- $\delta$  – displacement [mm];
- $b$  – specimen's width (25 mm);
- $a$  – crack length [mm];
- $\Delta$  - experimental calibration parameter based on the interception of the least squares plot of the cubic root compliance as a function of the measured crack length;
- $F$  – large displacement correction;
- $N$  – load-block correction.

Both  $F$  and  $N$  were calculated based on the ISO 25217 [6].

### 3. Results and Discussion

Figure 2 shows the representative load versus displacement curves of the specimens AF 163-2k [0/90<sub>2</sub>/AF163-2k/0]<sub>s</sub> (Fig. 2(a)) and Araldite [90/45/-45/AF163-2k/0]<sub>s</sub> (Fig. 2(b)), including their respective post-Morten fracture surfaces (Fig 2 (c) and (d)).

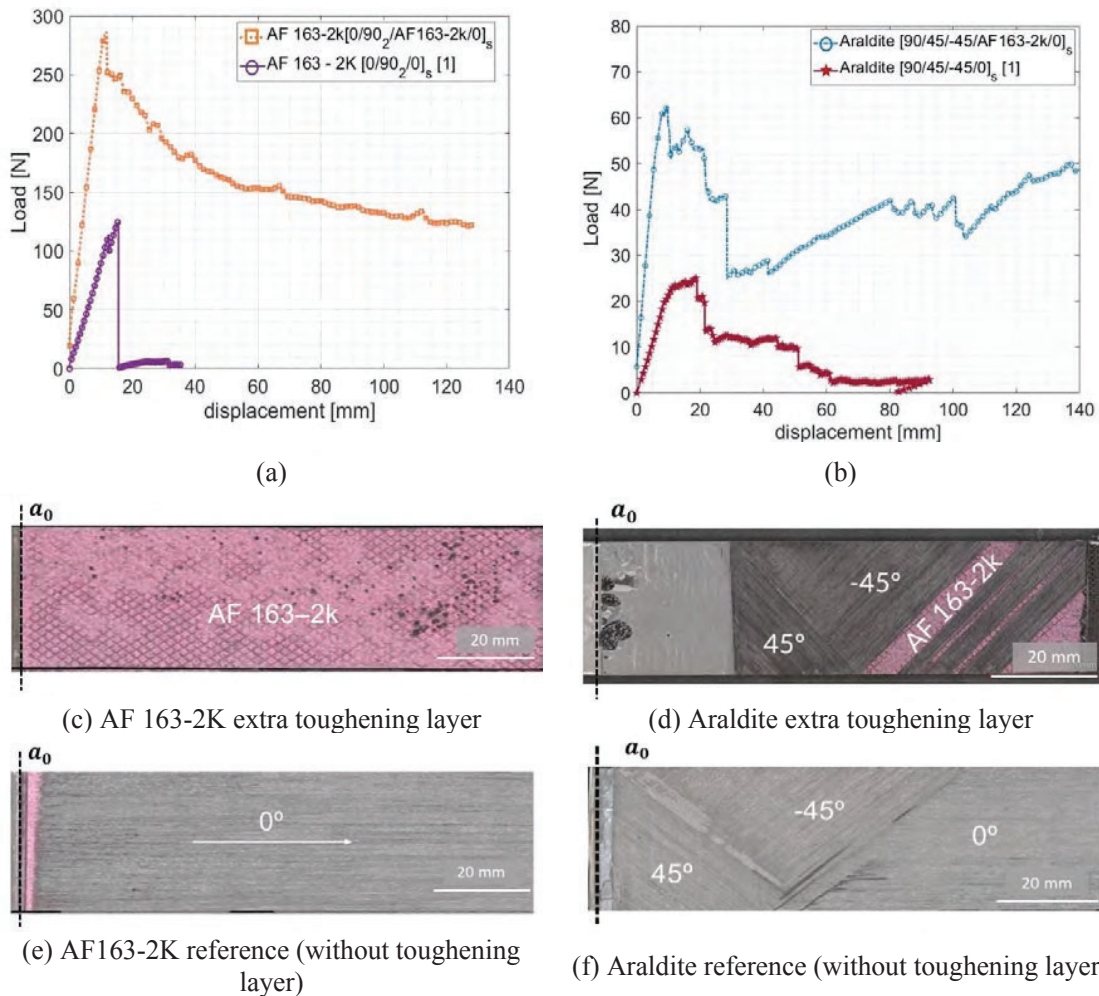


Figure 2: Representative load versus displacement curves of samples (a) AF 163-2k [0/90<sub>2</sub>/AF163-2k/0]<sub>s</sub> and AF 163-2k [0/90<sub>2</sub>/0]<sub>s</sub> and (b) Araldite [90/45/-45/AF163-2k/0]<sub>s</sub> and Araldite [90/45/-45/0]<sub>s</sub>, with and without the toughening layer, and the fracture surfaces of the samples (c) and (e) AF 163-2k and (d) and (f) Araldite with and without the co-cured extra toughening layer, respectively.

Fig. 2 (a) and (b) demonstrate that the co-cured toughening layer has increased the stiffness of both adhesively bonded composite joint types as they present a steeper linear part of the curves when compared to their references (without the toughening layer). Additionally, the maximum peak load value is higher than that of the baseline specimens - AF 163-2k [0/90<sub>2</sub>/0]<sub>s</sub> and Araldite [90/45/-45/0]<sub>s</sub>.

In particular, Figure 2 (b) shows a wavy shape of the load versus displacement curve until a sudden drop in the load values around 30 mm of the displacement for the specimen with the toughening layer and almost the same trend for the baseline specimen with a decline in the load values, around 20 mm of displacement. The main difference is that after the load drop, the load values from the specimen Araldite [90/45/-45/AF163-2k/0]<sub>s</sub> keep increasing until the final failure; meanwhile, the baseline specimen (Araldite [90/45/-45/0]<sub>s</sub>) presents a plateau region (around 25 to 50 mm of displacement) followed by a gradual decrease of the load values in function of the displacement due to the final delamination at the 0-degree layer (see Fig. 2 (f)).

The further increase in the load values for Araldite [90/45/-45/AF163-2k/0]<sub>s</sub> can be attributed to the crack propagation path reaching the co-cured toughening layer. At this point, the crack is delayed and deflected to alternating crack paths between the toughening layer and the -45-degree ply, as is clearly shown by the fracture surface presented in Fig. 2 (d).

The load versus displacement curve of specimen AF 163-2k [0/90<sub>2</sub>/AF163-2k/0]<sub>s</sub> exhibited smooth behaviour after crack propagation due to a cohesive failure, as seen in Fig. 2 (c). The cohesive failure occurred in the AF 163-2K at the specimen's mid-plane adhesive position. The baseline instead presented a significant decrease in the load values due to the final delamination at the 0-degree layer (see Fig. 2(e)).

Figure 3 shows the corresponding effective fracture toughness as a function of the crack length.

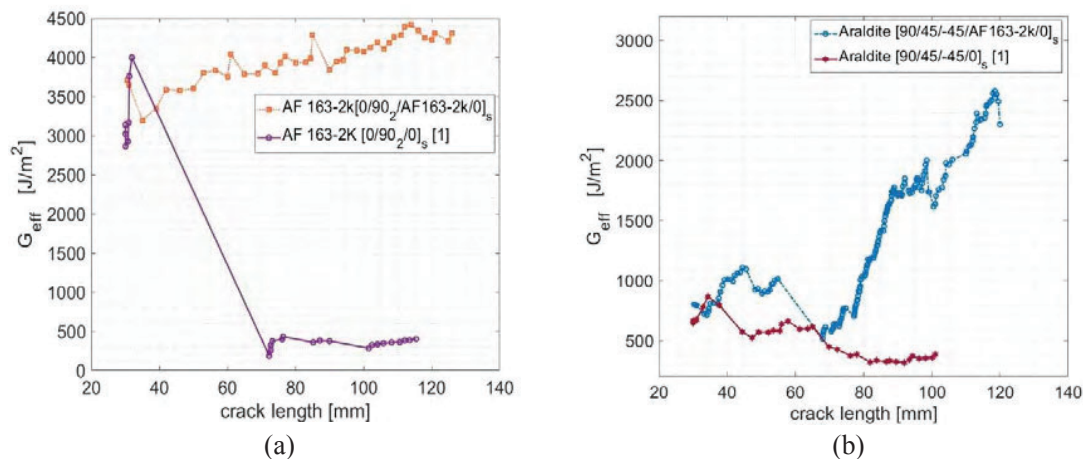


Figure 3: Effective fracture toughness of specimens bonded with (a) AF163-2K and (b) Araldite 2015, with and without the toughening layer.

As shown in Figure 3 (a), the highest peak of the effective onset fracture toughness is for the specimen without the toughening layer. The specimen with the co-cured toughening layer instead presents a smooth increase in the effective fracture toughness through the crack length. This behaviour can be associated with cohesive failure and carrier bridging, similar to what is observed in a unidirectional [0]<sub>s</sub> CFRP bonded with the AF 163-2k present in [1].

Figure 3 (b) shows similar values of the effective fracture toughness onset (around 600 J/m<sup>2</sup>) related to the beginning of the crack propagation within the adhesive layer. When the crack started to deflect through the composite thickness, a wavy shape was observed in both specimens, with a higher value for the Araldite [90/45/-45/AF163-2k/0]<sub>s</sub> with the toughening layer. Around 70mm of crack length, a significant increase is observed in the Araldite [90/45/-45/AF163-2k/0]<sub>s</sub> compared to its baseline. This increase in the R-curve slope was observed when the crack deflected from the -45 degree layer to the co-cured AF 163-2k layer, see Figure 4.

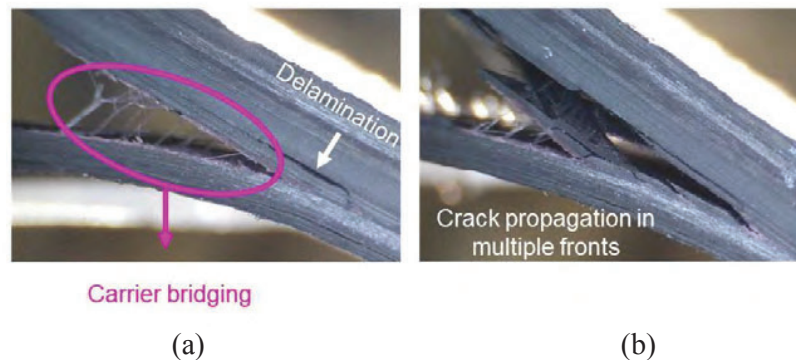


Figure 4: (a) First crack deflection to the co-cured toughening layer and (b) further deflection to the -45-degree layer of specimen Araldite [90/45/-45/AF163-2k/0]<sub>s</sub>.

As seen in Figure 4, when the crack deflected to the co-cured adhesive layer, the carrier triggered a crack bridging, holding the substrate's arms longer and delaying the crack propagation. The carrier bridging and the deflection of the specimen arms trigger different damage mechanisms (i.e. matrix cracking, fibre bridging and fibre/matrix debonding), and the crack deflects again to -45 degrees.

It is worth noting that a high deflection of the arms was observed when the crack reached the co-cured toughening layer. Therefore, further investigation is needed into the influence of the arms' flexibility on triggering different damage mechanisms and crack deflection between the laminate plies.

### 3. Conclusions

Adding a co-cured adhesive as a toughening layer is a promising solution to increase the effective joints' fracture toughness and delay crack propagation. Based on the study presented, the following conclusions could be drawn:

- The co-cured toughening layer has increased the stiffness and maximum peak load value of the adhesively bonded composite joint types;
- For the [0/90<sub>2</sub>/AF163-2k/0]<sub>s</sub> using a tough secondary bonded adhesive AF163-2k, the crack did not deflect as expected to the 0/90 crack plane and rather remained within the secondary bonded adhesive.
- For the [90/45/-45/AF163-2k/0]<sub>s</sub> using a low toughness secondary bonded adhesive, the presence of the toughening layer AF163-2K triggered a significant rise in the effective fracture toughness of the composite bonded joint (around 200% in 120 mm of crack length); The increase is caused by alternating crack path and crack deflections between the composite substrate and the toughening layer.

Further investigation is needed to study the influence of the arms' flexibility on triggering the different damage mechanisms and crack deflection between the laminate plies.

### Acknowledgements

The authors would like to acknowledge the PhD Candidate Michele Gulino for aiding in manufacturing the specimens.

The authors acknowledge Fundação para a Ciência e a Tecnologia (FCT) for its financial support via the project LAETA Base Funding (DOI: 10.54499/UIDB/50022/2020)

### References

- [1] R. A. A. Lima, R. Tao, A. Bernasconi, M. Carboni, N. Carrere, and S. Teixeira de Freitas, “Uncovering the toughening mechanisms of bonded joints through tailored CFRP layup,” *Compos B Eng*, vol. 263, Aug. 2023, doi: 10.1016/j.compositesb.2023.110853.
- [2] Araldite ® 2015-1 Two-component epoxy paste adhesive Key properties [Online], [www.aralditeadhesives.com](http://www.aralditeadhesives.com). [Accessed 6 May 2024].
- [3] J. Kupski, D. Zarouchas, and S. Teixeira de Freitas, “Thin-ply in adhesively bonded carbon fibre reinforced polymers,” *Compos B Eng*, vol. 184, p. 107627, 2020, doi: 10.1016/j.compositesb.2019.107627.
- [4] S. Teixeira de Freitas, D. Zarouchas, and J. A. Poulis, “The use of acoustic emission and composite peel tests to detect weak adhesion in composite structures,” *J Adhesion*, vol. 94, no. 9, pp. 743–766, 2018, doi: 10.1080/00218464.2017.1396975.
- [5] Lopes Fernandes R, Teixeira de Freitas S, Budzik MK, Poulis JA, Benedictus R. From thin to extra-thick adhesive layer thicknesses: fracture of bonded joints under mode I loading conditions. *Eng Fract Mech Sep*. 2019;218. <https://doi.org/10.1016/J.ENGFRACMECH.2019.106607>.
- [6] BS ISO 25217. Adhesives — determination of the mode I adhesive fracture energy of structural adhesive joints using double cantilever beam and tapered double cantilever beam specimens. 2009. <https://www.iso.org/standard/42797.html>. April, 2023.